ACS OMEGA

http://pubs.acs.org/journal/acsodf
Article

Improved Automated Radiosynthesis of [^{18}F]Dolutegravir: Toward Clinical Applications

Steve Huvelle, Antoine Pinon, Christine Coulon, Thomas Bonasera, Catherine Chapon, Thibaut Naninck, Roger Le Grand, Chris M. Parry, Bertrand Kuhnast, and Fabien Caillé*

Cite This: *ACS Omega* 2024, 9, 41732−41741
Read Online

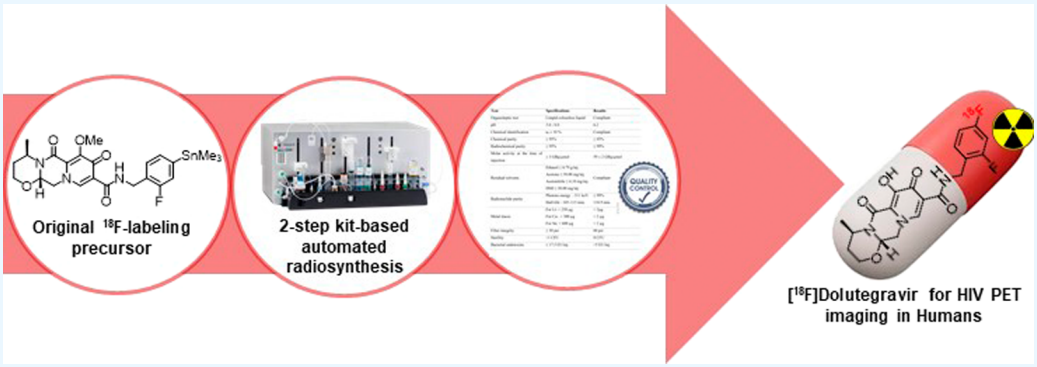

ABSTRACT: Positron emission tomography imaging using radiolabeled dolutegravir (DTG) is an interesting approach to understand the biodistribution of this antiretroviral drug at HIV-1 sanctuary sites. In the course of clinical translation, we depict herein an improved and pharmaceutically compliant radiosynthesis of [^{18}F]DTG from an original tin precursor. The radiosynthesis was achieved in two steps by copper-mediated radiofluorination, followed by enol ether deprotection using a kit-based AllInOne module. Ready-to-inject [^{18}F]DTG was obtained in 20 ± 5% (n = 12) decay-corrected radiochemical yield within 90 min, representing a 4-fold increase compared to the previously published three-step radiosynthesis. Quality control was carried out with three consecutive [^{18}F]DTG productions according to the current European Pharmacopoeia guidelines, which include pH determination, identity and purity (chemical, radiochemical, and radionuclide) assessments, residual solvent quantification, dosage of lithium, copper, and tin traces, sterility and bacterial endotoxin tests. [^{18}F]DTG (∼2 GBq) was obtained with a molar activity of 59 ± 2 GBq/μmol at the time of injection and was suitable for human applications.

INTRODUCTION

Dolutegravir (Tivicay, DTG) is an antiretroviral (ARV) drug approved by the FDA in 2013 for the treatment of human immunodeficiency virus (HIV-1).[1] DTG is a second-generation integrase strand transfer inhibitor (INSTI) which prevents proviral DNA from incorporating into the genome of CD4$^+$ cells, thus blocking the viral replication cycle and limiting virus propagation.[2] Used in combination with reverse-transcriptase inhibitors like tenofovir and emtricitabine, DTG is part of the combined antiretroviral therapy (cART) recommended by the World Health Organization.[3−5] With improved virological control compared to first-generation INSTIs such as raltegravir,[6] DTG made virological control a more achievable goal for patients treated with cART. However, all infected cells are not eliminated by cART with remaining viral reservoirs within pharmacological sanctuaries where the exposure to ARV drugs may be suboptimal.[7,8] Understanding the interactions of ARVs such as DTG with the virus and its microenvironment within these reservoirs is a key challenge to tackle as we move toward longer-term treatments and eventually remission or cure.[9]

Positron emission tomography (PET) is a state-of-the-art molecular imaging technique to quantitatively assess pharmacokinetic parameters of drug distribution in tissues with high sensitivity. PET imaging using radiolabeled ARV drugs is therefore an interesting approach to explore the distribution of these drugs in the sanctuary sites where virus reservoirs remain. This approach has been exemplified with fluorine-18-labeled raltegravir in an early phase 1 clinical trial (NCT03174977). With two fluorine atoms on its scaffold, DTG can be isotopically labeled with fluorine-18 (β^+, $t_{1/2}$ = 109.8 min),

Received: June 25, 2024
Revised: September 12, 2024
Accepted: September 17, 2024
Published: September 27, 2024

https://doi.org/10.1021/acsomega.4c05893
ACS Omega 2024, 9, 41732−41741

Scheme 1. Comparing the Three-Step Radiosynthesis of [^{18}F]DTG[10] with the Late-Stage Fluorination Depicted Herein

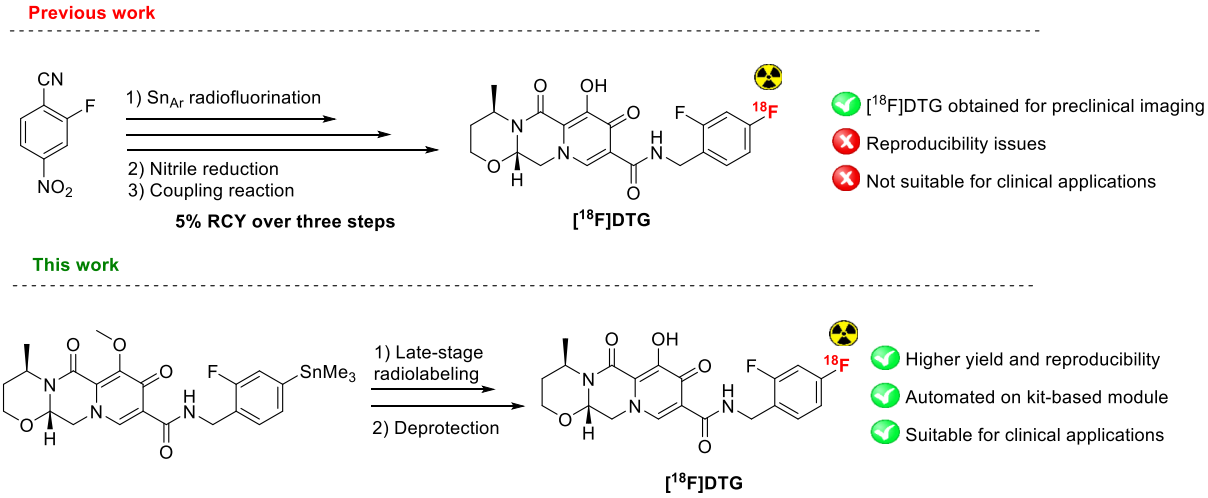

Scheme 2. Synthesis of the Protected Trimethyltin Precursor2 from Compound GSK3210346A[a]

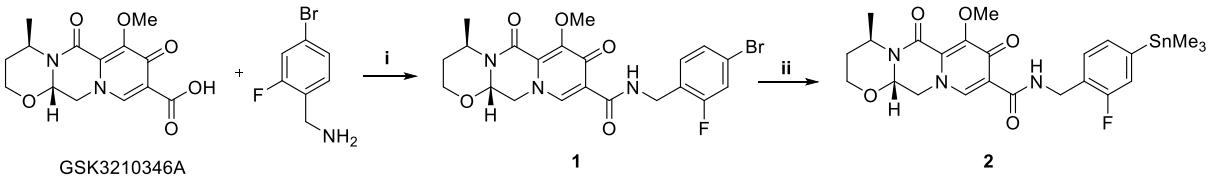

[a]Reagents and conditions: (i) TBTU, DIPEA, DMF, r.t. 16 h, 90% ; (ii) Sn_2Me_6, $Pd(PPh_3)_4$, 1,4-dioxane/Et_3N (3/1 v/v), 110 °C, 1 h, 85%.

Scheme 3. Deprotection of the Enol Ether Moiety of Compound 3 in DMI to Afford DTG

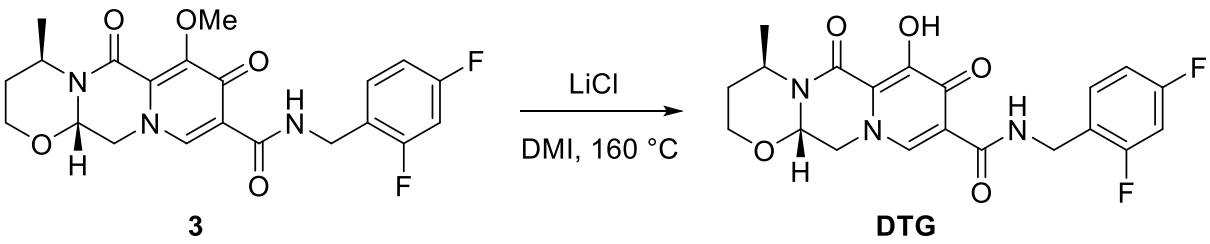

i.e., without modification of the chemical and biological properties of the drug. We have recently described the radiosynthesis of [^{18}F]DTG and the first *in vivo* PET imaging of this radiotracer in a healthy non-human primate.[10] Although this approach afforded [^{18}F]DTG in *ca.* 5% radiochemical yield (RCY) and sufficient purity and molar activity (MA) to perform preclinical imaging, this radiosynthesis was not suitable for translational perspectives toward clinical imaging. Indeed, this approach involves a three-step radiosynthesis from 2-fluoro-4-nitrobenzonitrile including a reduction of the nitrile function using nickel boride (Scheme 1). This reduction is very sensitive to stoichiometry, and defluorination is observed. Moreover, this reduction generates insoluble Ni(0) species capable of clogging the module tubing, thus increasing the risk of synthesis failure. In parallel, our first attempts to radiolabel DTG by late-stage fluorination using copper-assisted approaches[11] from a tributyltin precursor were unsuccessful.[10] Recent literature[12−14] demonstrated that using trimethyltin precursors instead of tributyltin and 1,3-dimethyl-2-imidazolidinone (DMI) as solvent instead of dimethylformamide (DMF) greatly improves the radiofluorination of stannanes. Taking into account these new considerations, we decided to develop a new late-stage approach for the radiolabeling of DTG and clinical translation (Scheme 1). Herein we describe the synthesis of a trimethyltin derivative of DTG with a methyl enol ether protective group. This precursor was submitted to late-stage radiolabeling with fluorine-18 followed by deprotection of the enol ether to afford [^{18}F]DTG. After optimization was carried out on a TRACERlab FX N Pro synthesizer, the whole process was automated on a kit-based AllInOne synthesizer for clinical applications. The radiotracer production was submitted to full quality control including radio-HPLC, residual solvents measurements by gas chromatography and HPLC, quantitative determination of residual metal traces (Li, Cu, and Sn) by inductively coupled plasma optical emission spectrometry (ICP-OES), and bioburden and sterility testing according to the current European Pharmacopoeia recommendations to ensure its suitability for human use.

RESULTS AND DISCUSSION

Chemistry. The synthesis of precursor **2** was carried out in two steps from compound GSK3210346A[15] (Scheme 2). A coupling reaction with commercially available 2-fluoro-4-bromobenzylamine in the presence of 2-(*1H*-benzotriazole-1-yl)-1,1,3,3-tetramethylaminium tetrafluoroborate (TBTU) and diisopropylethylamine (DIPEA) afforded bromo derivative **1**

https://doi.org/10.1021/acsomega.4c05893
ACS Omega 2024, 9, 41732−41741

in a 90% yield. A palladium-catalyzed stannation reaction with hexamethylditin afforded the protected precursor **2** in an 85% yield. Demethylation of the enol ether moiety of **2** following the method of Budidet *et al.*[15] failed. Therefore, we considered a two-step radiosynthesis directly from **2** involving a radiofluorination step, followed by the enol ether deprotection.

Optimization of the demethylation of methyl DTG **3**[15] using lithium chloride was studied (Scheme 3). Because the radiofluorination step will be carried out in DMI, this solvent was selected. Optimization of the reaction conditions, *i.e.*, the quantity of lithium chloride and the reaction time, was achieved at 160 °C, and the conversion of the reaction was measured by liquid chromatography/mass spectroscopy (LC/MS) (Table 1) (see Figure S5 in the Supporting Information).

Table 1. Optimization of the Reaction Conditions for the Deprotection of the Enol Ether Moiety of 3 Performed in DMI at 160 °C

entry[a]	LiCl equivalents	reaction time (min)	conversion (mean ± SD %)[b]
1	10	5	77 ± 1
2		10	95.5 ± 0.5
3		15	98.5 ± 0.5
4	20	5	95.5 ± 0.5
5		10	97 ± 0
6		15	100 ± 0
7	**50**	**5**	**100 ± 0**

[a]Experiments were performed in duplicate. [b]Conversion was measured by LC/MS with UV detection as the ratio of the AUC of the DTG peak over the sum of the AUC of all peaks. Conversion is the mean of two experiments.

In the presence of 5 equiv of lithium chloride, DTG was obtained in 77% conversion after 5 min (Table 1, entry 1). Increasing the reaction time to 10 and 20 min led to conversions of 95.5% and 98.5%, respectively (Table 1, entries 2 and 3). In order to reach full conversion, the quantity of lithium chloride was increased to 20 equiv. After 5 min, the DTG conversion reached 95.5% (Table 1, entry 4). Full conversion was obtained after 20 min of reaction (Table 1, entry 6). Keeping in mind the short half-life of fluorine-18 ($t_{1/2}$ = 109.8 min), the amount of lithium chloride was further increased to 50 equiv in order to accelerate the reaction. Full conversion was obtained under those conditions after 5 min (Table 1, entry 7).

Radiochemistry. With optimized conditions in hand for the deprotection reaction, we decided to explore the radiofluorination of precursor **2** with $[^{18}F]F^-$, inspired by the copper-mediated protocol described by Makaravage *et al.*[11] (Scheme 4). Optimization of the reaction conditions, *i.e.*, quantity of the precursor, number of equivalents of the Cu(II) complex compared to precursor **2**, and reaction temperature, was performed on a TRACERlab FX N Pro module (Table 2).

Table 2. Optimization of the Copper-Mediated Radiofluorination of Precursor2 Performed in DMI on a TRACERlab FX N Pro Module

entry[a]	quantity of 2	equivalents of $Cu(OTf)_2Py_4$	reaction conditions	conversion (mean ± SD %)[b]
1	4 mg	2.5	110 °C, 20 min (sequential addition of **2**) and Cu(OTf)2Py4	3.3 ± 0.3
2	4 mg	2.5	110 °C, 20 min	25 ± 1
3	4 mg	2.5	140 °C, 20 min	25.5 ± 0.5
4	4 mg	4	110 °C, 20 min	25 ± 0.5
5	4 mg	1	110 °C, 20 min	14 ± 2
6	**2 mg**	**2.5**	110 °C, 20 min	**29 ± 0**
7	1 mg	2.5	110 °C, 20 min	11.3 ± 0.8

[a]Experiments were performed in duplicate. [b]Conversion was measured by radio-TLC as the ratio of the AUC of $[^{18}F]$**3** over the sum of the AUC of all peaks. Conversion is the mean of two experiments.

Prior to radiofluorination, cyclotron-produced $[^{18}F]F^-$ was trapped on a quaternary methylammonium (QMA) cartridge, eluted with a solution of potassium triflate and potassium carbonate in a mixture of acetonitrile and water, and azeotropically dried. Radiofluorination was performed in DMI. The conversion of the reaction was measured by thin-layer chromatography with gamma detection (radio-TLC) (see Figure S6 in the Supporting Information). Following a recent procedure in the literature,[16] radiofluorination was first performed with 4 mg of precursor **2** and 2.5 equiv of the Cu(II) complex at 110 °C for 20 min, with sequential addition of a solution of **2** in DMI followed by a solution of $Cu(OTf)_2Py_4$ in DMI (Table 2, entry 1). In those conditions, a low conversion of 3.3% was observed. Performing the reaction in the same conditions but with a premixed solution of **2** and $Cu(OTf)_2Py_4$ in DMI led to a significant increase of the conversion to 25%, comparable to the results depicted by Makaravage *et al.* with electron-rich arenes (Table 2, entry 2).[11] Premixing the [Cu] complex with the trimethyl tin precursor seems to be important to perform the first oxidative addition step and allows for a rapid reaction with fluorine-18. Increasing the reaction temperature to 140 °C or the quantity of $Cu(OTf)_2Py_4$ did not lead to an improved conversion (Table 2, entries 3 and 4), whereas reducing the quantity of the Cu(II) complex to 1 equiv compared to **2** resulted in a decreased conversion of 14% (Table 2, entry 5). In contrast, reducing the quantity of **2** to 2 mg resulted in a 29% conversion (Table 2, entry 6). These conditions enable us to

Scheme 4. Copper-Mediated Radiofluorination of Precursor2 to Form Methyl DTG $[^{18}F]$3

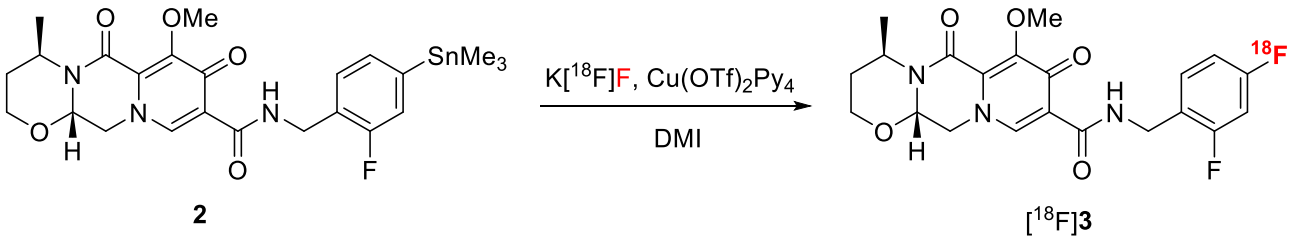

2 $[^{18}F]$**3**

https://doi.org/10.1021/acsomega.4c05893
ACS Omega 2024, 9, 41732−41741

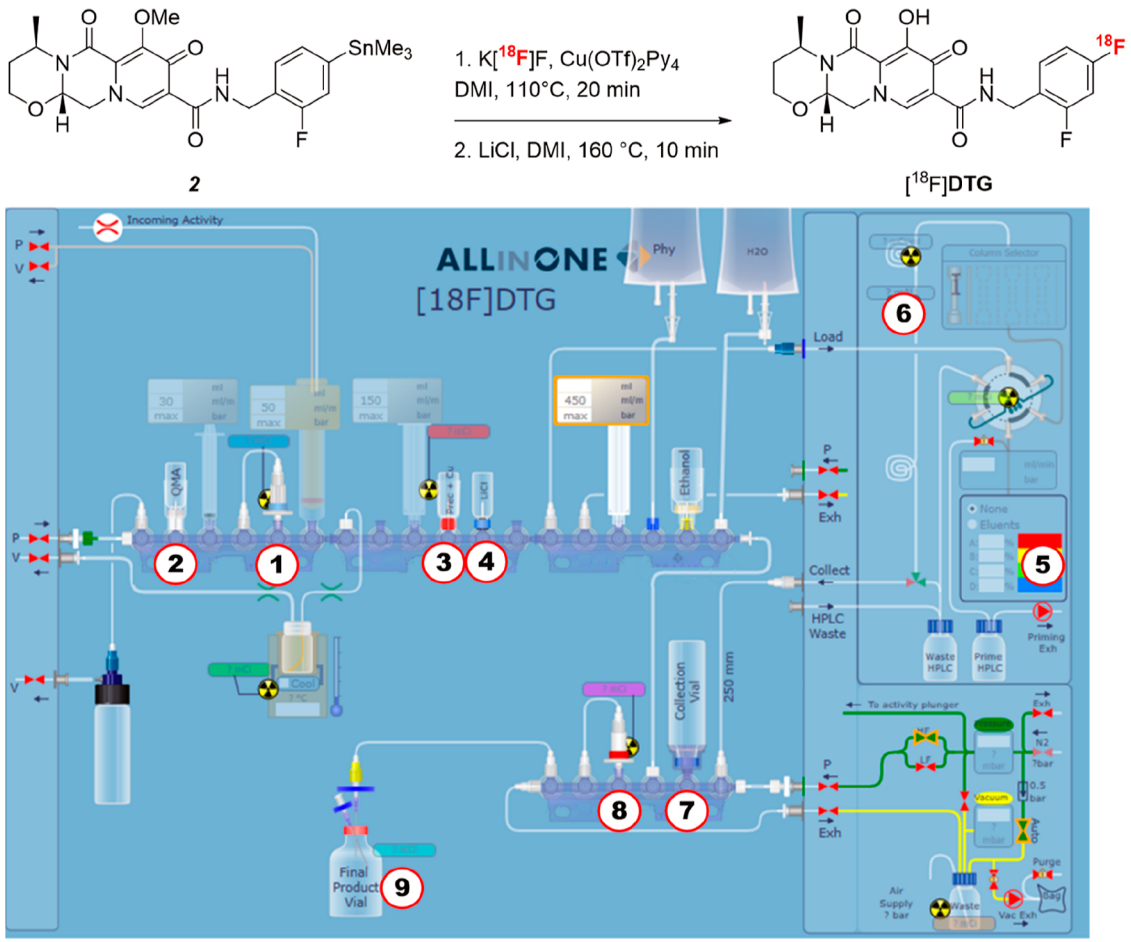

Figure 1. Synopsis of the one-pot [^{18}F]DTG radiosynthesis performed on a Trasis AIO synthesizer. (1) QMA cartridge; (2) QMA elution solution: 500 μL of CH_3CN, 450 μL of a solution of KOTf in water (10 mg/mL), and 50 μL of an aqueous solution of K_2CO_3 (1 mg/mL); (3) solution of **2** (2 mg) and $Cu(OTf)_2Py_4$ (6 mg) in 550 μL of DMI; (4) solution of LiCl (7.5 mg) in 350 μL of DMI; (5) HPLC eluent: H_2O/CH_3CN/TFA (65/35/0.1 v/v/v); (6) HPLC column: Waters Symmetry (C18 7.8 × 300 mm, 7 μm); (7) collection vial filled with 35 mL of H_2O; (8) AttractSPE HLB 30 mg cartridge; (9) final product vial recovering [^{18}F]DTG in 1.5 mL of ethanol and 13.5 mL of 0.9 wt % $NaCl_{aq}$.

spare some precursor and were chosen for the automated radiosynthesis of [^{18}F]DTG. Lower quantities of **2** (1 mg) led to a decreased conversion of 11.3% (Table 2, entry 7).

The automated two-step radiosynthesis of [^{18}F]DTG was performed on a Trasis AllInOne (AIO) synthesizer by using the optimized conditions depicted above (Figure 1). This module fully operates with disposable kits to avoid cross-contamination and is perfectly suitable for the production of radiopharmaceuticals for human use. Cyclotron-produced [^{18}F]F^- was trapped on a QMA cartridge, and elution to the reactor was performed with a KOTf/K_2CO_3 solution in acetonitrile and water. The resulting K[^{18}F]F complex is dried at 125 °C under vacuum. Although the presence of water is deleterious for radiofluorination, it is interesting to note that this drying sequence was sufficient and performing an additional step of coevaporation with acetonitrile did not improve the yield. After addition of the solution of **2** (2 mg) and $Cu(OTf)_2Py_4$ (2.5 equiv) in DMI, radiofluorination was carried out at 110 °C for 20 min according to the optimized conditions determined above. Enol ether deprotection was performed by addition of a lithium chloride solution (50 equiv compared to **2**) in DMI. Fortunately, deprotection could be performed in one pot, simplifying the whole process. However, in contrast with the optimized conditions depicted above, 10 min were necessary to obtain [^{18}F]DTG with full conversion.

Purification by semi-preparative HPLC was carried out with a reverse-phase C18 column using water, acetonitrile, and trifluoroacetic acid (TFA) (Figure 2). Although prepurification on an Alumina N cartridge facilitates the elimination of unreacted [^{18}F]F^-, we also observed significant retention of [^{18}F]DTG on the cartridge. Therefore, the crude reaction mixture was directly injected in HPLC without prepurification. In order to obtain the ready-to-inject radiotracer for *in vivo* applications, a formulation step was carried out using solid-phase extraction (SPE) with a C18 cartridge to eliminate the acetonitrile used during the purification step. The radiotracer was formulated in a mixture of ethanol and physiological serum (1.5/13.5 v/v). Finally, ready-to-inject [^{18}F]DTG was obtained with 20 ± 5% (n = 12) RCY in 90 min. This represents a 4-fold increase in comparison with the previous three-step method we have described (5.1 ± 0.8% within 95 min).

Quality Control. The [^{18}F]DTG quality control was carried out on three successive batches according to the European Pharmacopoeia 11.5 monograph n°04/2023:0125. The results are presented in Table 3.[17] Analysis are depicted in the Supporting Information (Figures S7−S10). The [^{18}F]DTG solution was limpid and colorless at a pH of 6.2. Reverse-phase analytical HPLC confirmed the identity of [^{18}F]DTG, with the retention time within the t_R^{ref} ± 10% range (Figure 3). Both chemical and radiochemical purities were above 95%. To

https://doi.org/10.1021/acsomega.4c05893
ACS Omega 2024, 9, 41732−41741

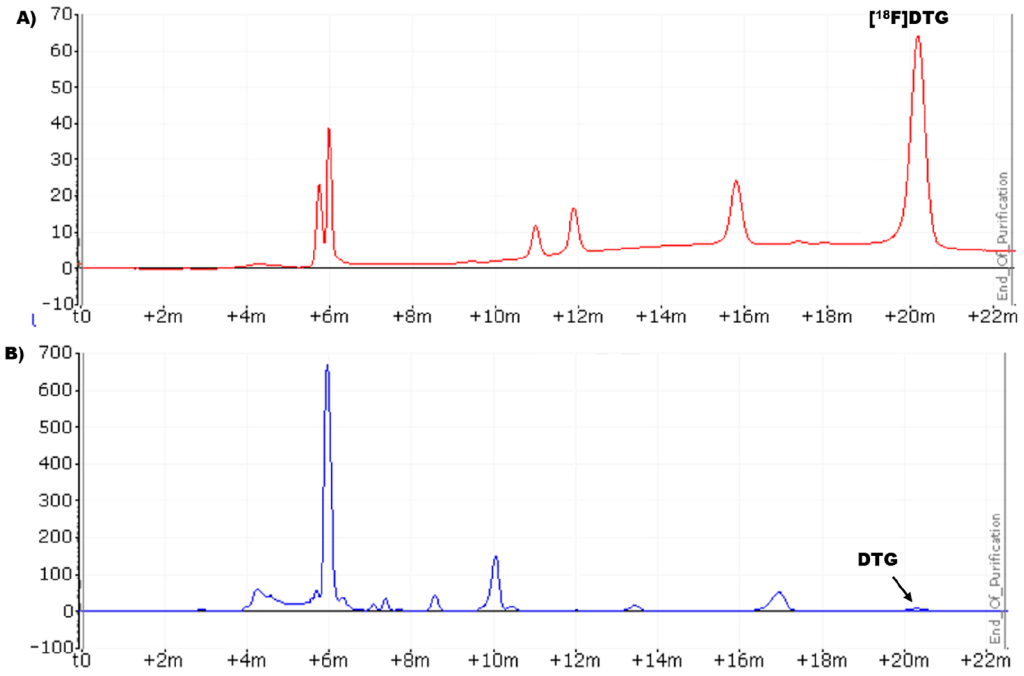

Figure 2. Purification of [^{18}F]DTG carried out by reverse-phase HPLC using UV (254 nm) and gamma detectors. (A) Gamma chromatogram; (B) UV chromatogram.

Table 3. [^{18}F]DTG Quality Control Following the Recommendations of the European Pharmacopoeia 11.5[17]

test	specifications[17]	results
organoleptic test	limpid colorless liquid	compliant
pH	5.0−8.0	6.2
chemical identification	t_R ± 10%	compliant
chemical purity	≥95%	≥95%
radiochemical purity	≥95%	≥99%
MA at the time of injection	≥3 GBq/μmol	59 ± 2 GBq/μmol
residual solvents	ethanol ≤ 0.79 g/inj	compliant
	acetone ≤ 50.00 mg/inj	
	acetonitrile ≤ 4.10 mg/inj	
	DMI ≤ 50.00 mg/inj	
radionuclide purity	photon energy: 511 keV	≥99%
	half-life: 105−115 min	110.9 min
metal traces	for Li: <250 μg	<2 μg
	for Cu: <300 μg	<2 μg
	for Sn: <600 μg	<2 μg
filter integrity	≥50 psi	60 psi
sterility	<1 CFU	0 CFU
bacterial endotoxins	≤17.5 EU/inj	<5 EU/inj

ensure that the [^{18}F]DTG final solution is in the tracer dose specifications for PET, we have set a maximum injected mass of DTG of 50 μg, a hundred times below the pharmacological dose prescribed (5 mg per pill).[18] This corresponds to a minimum MA of 3 GBq/μmol for a 350 MBq average injection in humans. The average MA measured for the [^{18}F]DTG batches is 59 GBq/μmol at the time of injection. Therefore, [^{18}F]DTG was considered to be in the tracer dose range. Gas chromatography was used to quantify the residual traces of acetonitrile and acetone in the final [^{18}F]DTG batches as well as the quantity of ethanol as an excipient, and the results were compliant with the European Pharmacopoeia specifications. Considering the high boiling point of DMI, this solvent could not be detected by static headspace gas chromatography. Instead, HPLC analysis with UV detection at 220 nm was performed. Using a calibration curve, an average concentration of 360 μg/inj of DMI was found in the [^{18}F]DTG batches. DMI is not carcinogenic and can be considered as a class 3 solvent. An acute toxicity of 2.84 g/kg was reported in mice,[19] which would correspond to a quantity of 170 g/inj for a 60 kg human being, *ca.* 500 times higher than the residual quantity of DMI found in the [^{18}F]DTG batches. As a result, this residual quantity of DMI was considered to be compliant with human injection. The radionuclide purity was above 99.9% with a half-life of 110.9 min, in the range of 105−115 min for fluorine-18 defined by the pharmacopoeia. Lithium (contained in the lithium chloride used for the deprotection reaction), copper (contained in the Cu(II) complex used for radiofluorination), and tin (contained in the precursor) were used during the radiopharmaceutical preparation. These metals are class 3 agents that require consideration in the risk assessment for the parenteral route as they are intentionally added.[20] It has been established that the exposure limit by parenteral routes for Li, Cu, and Sn were 250, 300, and 600 μg/day, respectively.[20] In our three batches of [^{18}F]DTG, Li, Cu, and Sn traces measured by ICP-OES were all below the detection limit of 0.2 μg/mL. This means that, for a 10 mL injection, the Li, Cu, and Sn traces are below 2 μg, more than a hundred times lower than the established limits for parenteral routes. The three [^{18}F]DTG batches are therefore considered non-toxic regarding the metal traces. Sterilization of the [^{18}F]DTG solution was performed with a 0.22 μm filter under a laminar flow hood. Integrity of the filter was verified by a bubble point test. Sterility was checked by incubation of the [^{18}F]DTG preparation for 13 days in resazurin thioglycolate, trypticase soy agar, and Sabouraud agar for aerobic and anaerobic bacteria, aerobic bacteria, and fungi, respectively. The level of bacterial endotoxins in the [^{18}F]DTG preparation, determined

https://doi.org/10.1021/acsomega.4c05893
ACS Omega 2024, 9, 41732−41741

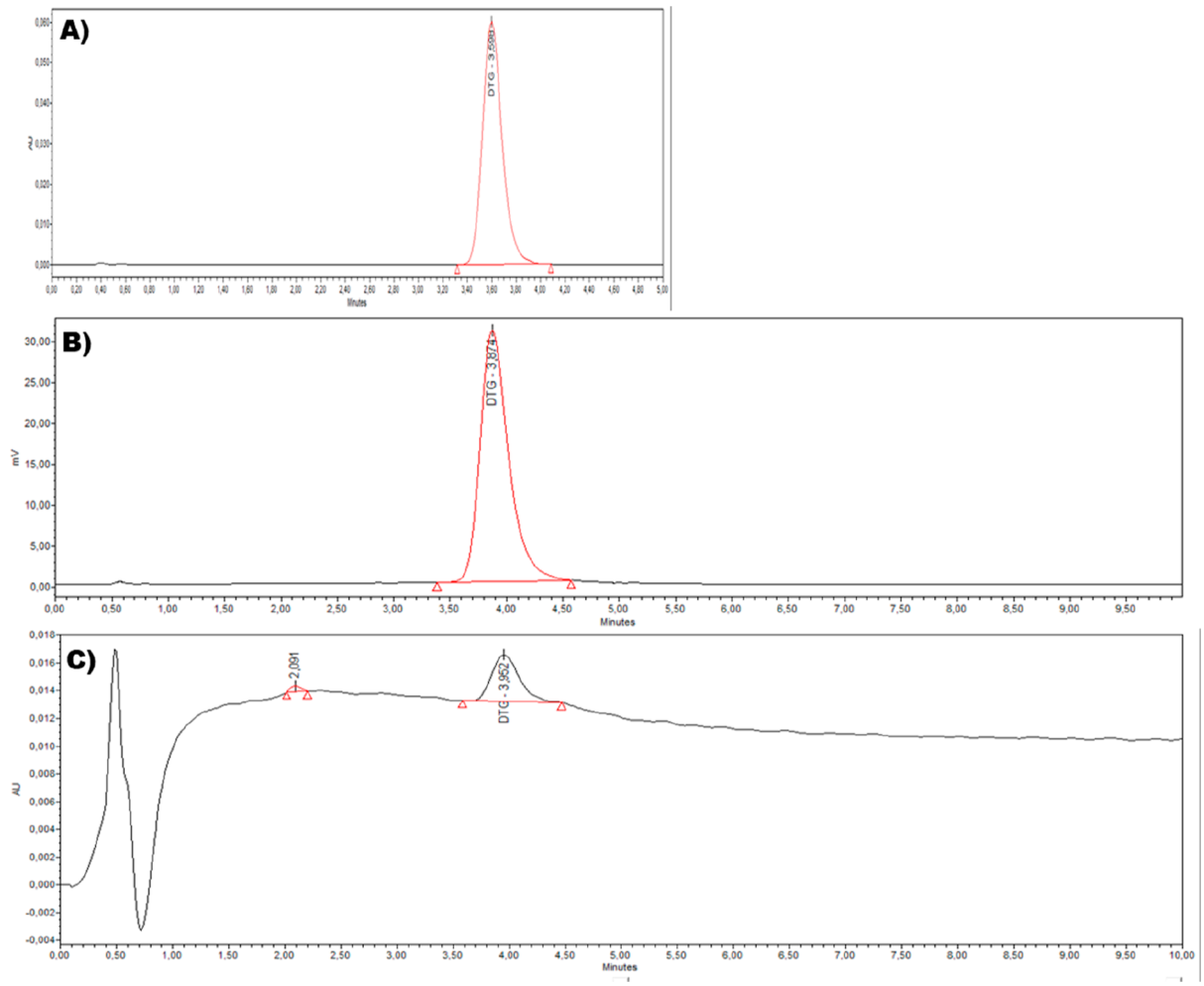

Figure 3. HPLC analysis of the ready-to-inject [^{18}F]DTG performed on a reverse-phase C18 column with UV (254 nm) and gamma detection. (A) Nonradioactive DTG reference (UV); (B) gamma chromatogram; (C) UV chromatogram.

with the Limulus amebocyte lysate (LAL) test, was under 5 EU/inj, below the limit of 17.5 EU/inj. In conclusion, the [^{18}F]DTG radiopharmaceutical preparation is declared suitable for human use, in accordance with the European Pharmacopoeia guidelines. Fifteen minutes were necessary to perform all the pre-release quality control operations, including pH measurement, the organoleptic test, identification, purity determination, and the filter integrity test. This amount of activity left for injection was *ca.* 2000 MBq of [^{18}F]DTG, whereas PET imaging in humans requires typically 300−400 MBq.

CONCLUSIONS

We have developed a new and more robust radiosynthesis of [^{18}F]DTG for clinical PET imaging of HIV. A trimethyltin precursor with a methyl-protected enol moiety was synthesized in two steps. The deprotection of the enol ether was optimized under non-radioactive conditions to reach full conversion rapidly. The copper-mediated radiofluorination of the trimethyltin precursor was optimized on a TRACERlab FX N Pro module, and the whole radiosynthesis process was automated on a kit-based pharmaceutically compliant AllInOne module. Ready-to-inject [^{18}F]DTG was obtained in 20 ± 5% RCY (n = 12) with a 4-fold increase compared to the previous three-step radiosynthesis of the literature. Full quality control according to the European Pharmacopoeia guidelines was performed to demonstrate that [^{18}F]DTG production can be used for human injection.

MATERIALS AND METHODS

Chemistry. Chemicals were purchased from Aldrich and used as received. GSK provided dolutegravir and compound GSK3210346A. Thin-layer chromatography (TLC) on aluminum-precoated plates of silica gel 60F254 (VWR, France) was used to monitor reactions, and compounds were localized using a UV lamp at 254 nm. ^{1}H and ^{13}C NMR spectra were recorded on an ADVANCE 400 MHz apparatus (Bruker, France). $CDCl_3$ was used as the deuterated solvent. Chemical shifts (δ) are reported in ppm (s, d, t, q, and b for singlet, doublet, triplet, quadruplet, and broad signal, respectively) with the solvent residual chemical shift as reference. Ultra-performance liquid chromatography−mass spectroscopy (UPLC−MS) was performed on an Ultimate 3000 (Thermo Scientific, USA) device equipped with an ACQUITY BEH 2.1 × 50 mm, 1.7 μm column (Waters, USA). A gradient of water with 0.1% formic acid and acetonitrile with 0.1% formic acid (3% CH_3CN/HCHO for 2 min, then rising to 100% for 7 min, then decreasing to 3% for 1 min, and then keeping 3% for 2 min) at a flow rate of 0.3 mL/min was used. Mass spectroscopy was performed with a Linear Trap Quadrupole

https://doi.org/10.1021/acsomega.4c05893
ACS Omega 2024, 9, 41732−41741

Orbitrap Velos (Thermo Scientific, USA) equipped with an electron spray ionization (ESI) chamber. Spectra were recorded between 100 and 1000 m/z. High-resolution mass spectroscopy (HRMS) was performed on a Bruker maXis mass spectrometer by the SALSA platform from the ICOA laboratory.

(4*R*,12a*S*)-*N*-(4-Bromo-2-fluorobenzyl)-7-methoxy-4-methyl-6,8-dioxo-3,4,6,8,12,12a-hexahydro-2*H*-pyrido-[1′,2′:4,5]pyrazino[2,1-*b*][1,3]oxazine-9-carboxamide (1). Compound GSK3210346A (650 mg, 1.84 mmol, 1.5 equiv) and TBTU (591 mg, 1.84 mmol, 1.5 equiv) were stirred in anhydrous DMF (13 mL) at room temperature for 2 min before DIPEA (320 μL, 1.84 mmol, 1.5 equiv) and 4-bromo-2-fluorobenzylamine (250 mg, 1.23 mmol, 1.0 equiv) were added. The resulting mixture was stirred at room temperature under an argon atmosphere for 16 h. The solution was diluted with EtOAc (10 mL) and washed successively with aqueous solutions of HCl 1 M (10 mL), $NaHCO_{3(sat)}$ (20 mL), LiCl (5 wt %/v, 20 mL), and brine (10 mL). The organic layer was dried over Na_2SO_4, filtered, and concentrated. The crude residue was purified on silica gel using $MeOH/CH_2Cl_2$ (5/95 v/v) as an eluent to give compound **1** (550 mg, 90%) as a yellow powder. ^{1}H NMR (400 MHz, $CDCl_3$): δ 10.40 (t, J = 5.9 Hz, 1H), 8.41 (s, 1H), 7.24−7.19 (m, 3H), 5.18 (dd, J = 6.1 Hz, J = 3.8 Hz, 1H), 4.99 (dd, J = 6.9 Hz, J = 1.9 Hz, 1H), 4.59 (d, J = 6.0 Hz, 2H), 4.28 (dd, J = 13.5 Hz, J = 3.8 Hz, 1H), 4.12 (dd, J = 13.4 Hz, J = 6.2 Hz, 1H), 4.00 (s, 3H), 3.94 (dd, J = 8.8 Hz, J = 2.2 Hz, 2H), 2.21−2.11 (m, 1H), 1.51 (dd, J = 14.0 Hz, J = 2.2 Hz, 1H), 1.33 (d, J = 7.0 Hz, 3H) ppm. ^{13}C NMR (101 MHz, $CDCl_3$): δ 174.6, 164.2, 161.0 (d, J = 251.3 Hz), 155.7, 154.7, 142.3, 130.8 (d, J = 4.9 Hz), 129.3, 127.5(d, J = 3.7 Hz), 124.8 (d, J = 15.0 Hz), 121.2 (d, J = 9.4 Hz), 119.2, 118.9, 76.2, 62.6, 61.2, 53.5, 44.6, 36.7 (d, J = 4.0 Hz), 29.5, 16.1 ppm. HR-ESI(+)-MS m/z calcd for $C_{21}H_{22}FBrN_3O_5$, 494.0721 $[M + H]^+$; found, 494.0719.

Analyses were in accordance with the literature.[10]

(4*R*,12a*S*)-*N*-(2-Fluoro-4-(trimethylstannyl)benzyl)-7-methoxy-4-methyl-6,8-dioxo-3,4,6,8,12,12a-hexahydro-2*H*-pyrido[1′,2′:4,5]pyrazino[2,1-*b*][1,3]oxazine-9-carboxamide (2). Compound **1** (201 mg, 0.407 mmol, 1.0 equiv), hexamethylditin (200 mg, 0.61 mmol, 1.5 equiv), $Pd(PPh_3)_4$ (94 mg, 0.08 mmol, 0.2 equiv), and a 1,4-dioxane/trimethylamine mixture (4 mL, 3/1 v/v) were added in a sealed tube and stirred under argon at 110 °C for 1 h. The suspension was concentrated under reduced pressure, and the residue was purified by column chromatography ($MeOH/CH_2Cl_2$ 5/95 v/v) to afford compound **2** (200 mg, 85%) as a yellow solid. ^{1}H NMR (400 MHz, $CDCl_3$): δ 10.34 (t, J = 5.6 Hz, 1H), 8.39 (s, 1H), 7.34 (t, J = 7.2 Hz, 1H), 7.16 (dd, J = 12.6 Hz, J = 8.3 Hz, 2H), 5.19 (dd, J = 6.2 Hz, J = 3.8 Hz, 1H), 5.05−4.94 (m, 1H), 4.65 (d, J = 5.8 Hz, 2H), 4.26 (dd, J = 13.4 Hz, J = 3.8 Hz, 1H), 4.11 (dd, J = 13.4 Hz, J = 6.2 Hz, 1H), 4.02 (s, 3H), 3.96 (dd, J = 8.7 Hz, J = 2.0 Hz, 2H), 2.23−2.13 (m, 1H), 1.52 (dd, J = 14.0 Hz, J = 2.1 Hz, 1H), 1.35 (d, J = 7.0 Hz, 3H), 0.27 (s, 9H) ppm. ^{13}C NMR (101 MHz, $CDCl_3$): δ 174.6, 164.0, 160.8 (d, J = 251.4 Hz), 155.8, 154.8, 142.2, 131.6 (d, J = 3.7 Hz), 129.4 (d, J = 3.3 Hz), 129.2, 125.2 (d, J = 15.0 Hz), 122.1 (d, J = 17.8 Hz), 119.2, 76.3, 62.6, 61.2, 53.6, 44.6, 37.2, 29.5, 16.2, −9.4 ppm. HR-ESI(+)-MS m/z calcd for $C_{24}H_{31}FN_3O_5Sn$, 580.1264 $[M + H]^+$; found, 580.1264 (see Figures S1−S3 in the Supporting Information for NMR and LC/MS analysis).

Optimization of Enol Ether Deprotection. Compound **3** (4 mg, 1 equiv) was dissolved in DMI (800 μL) and different quantities of LiCl (4, 8, or 19 mg, 10, 20, or 50 equiv, respectively) were added. The reaction mixture was heated at 160 °C for 5, 10, or 15 min. The crude was analyzed by LC/MS/UV (254 nm). The conversion of **3** into DTG was measured as the ratio of the AUC of the DTG peak over the sum of the AUCs of all of the peaks on the UV chromatogram.

Radiochemistry. *General Information.* All reactions were carried out using a TRACERlab FX N Pro module (GE Healthcare, Sweden) or an AllInOne module (Trasis, Belgium). No carrier-added [^{18}F]fluoride ion was produced *via* the ^{18}O(p, n)^{18}F nuclear reaction by irradiation of a 2 mL [^{18}O]water (>97% enriched, Rotem, Israël) target with an IBA Cyclone 18/9 (IBA, Belgium) cyclotron.

The radiochemical yield was measured as the ratio of the final radioactivity of the ready-to-inject radiotracer measured in an activity chamber (Capintec, Berthold, France) over the starting activity of the [^{18}F]fluoride anions measured in a gamma counter of the synthesizer upon reception from the cyclotron. The RCY was decay-corrected.

Optimization of Radiofluorination Affording [^{18}F]3. Radiosynthesis was carried out using a TRACERlab FX N Pro module (GE Healthcare, Sweden). [^{18}F]F^- (9−15 GBq) was trapped on an ion-exchange resin QMA light (Waters, USA) and eluted with a mixture of 500 μL of CH_3CN, 450 μL of an aqueous solution of KOTf (10 mg/mL), and 50 μL of an aqueous solution of K_2CO_3 (1 mg/mL). The resulting complex was dried upon heating at 60 °C for 7 min under vacuum and a stream of helium followed by heating at 120 °C for 5 min under vacuum only. The reactor temperature was decreased to 50 °C before 500 μL of CH_3CN were added. The mixture was heated to 100 °C under vacuum for 5 min to remove all traces of water. This procedure was repeated twice. Upon cooling to 70 °C, a solution of **2** (1−4 mg, 1.8−6.9 μmol) and $Cu(OTf)_2Pyr_4$ (3−12 mg, 4.9−17.3 μmol) in 500 μL of DMI was added and the mixture was heated at 110 °C for 20 min. Upon cooling to room temperature, the mixture was diluted with CH_3CN/H_2O (4 mL) and the crude product was analyzed by HPLC according to the HPLC analysis procedure of the quality control for chemical identification (see below). The radiochemical conversion was measured by radio-TLC performed on precoated plates of silica gel 60F254 (Merck, USA) and eluted with a mixture of dichloromethane/methanol (8/2 v/v). Radioactive compounds were detected using a MiniScan and Flow-Count radioactive detection system (Bioscan, France) operated with the Chromeleon software (Thermo Scientific, USA).

Fully Automated Radiosynthesis of [^{18}F]DTG on AIO. Radiosynthesis was carried out using an AIO module (Trasis, Belgium). [^{18}F]F^- (26−28 GBq) was trapped on an ion-exchange resin QMA light (Waters, USA) and eluted with a mixture of 500 μL of CH_3CN, 450 μL of an aqueous solution of KOTf (10 mg/mL), and 50 μL of an aqueous solution of K_2CO_3 (1 mg/mL). The resulting complex was dried upon heating at 125 °C for 3 min, followed by heating at 95 °C for 3 min under vacuum and a stream of helium. Upon cooling to 70 °C, a solution of **2** (2 mg, 3.5 μmol, 1.0 equiv) and $Cu(OTf)_2Py_4$ (6 mg, 9.7 μmol, 2.5 equiv) in 550 μL of DMI was added and the mixture was heated at 110 °C for 20 min. The mixture was cooled down to 70 °C before LiCl (7.5 mg, 177 μmol, 50.0 equiv) in 350 μL of DMI was added to the reactor. The mixture was heated for 10 min at 160 °C. Upon

https://doi.org/10.1021/acsomega.4c05893
ACS Omega 2024, 9, 41732−41741

cooling to room temperature, the mixture was diluted with H_2O (4 mL) and the crude was purified by reverse-phase semipreparative HPLC (Waters Symmetry C18 7.8 × 300 mm, 7 μm) equipped with an HPLC pump (Trasis, Belgium) using a mixture of H_2O/CH_3CN/TFA (65/35/0.1 v/v/v, 3.5 mL/min) as the eluent. UV detection was performed at 254 nm. The purified compound was diluted with water (35 mL) and passed through an AttractSPE HLB 30 mg cartridge (Affinisep, France). The cartridge was rinsed with water (20 mL) and eluted with ethanol (1.5 mL), and the final compound was diluted with saline (0.9% w/v, 13.5 mL). Ready-to-inject [^{18}F]DTG (2.2−3.7 GBq) was obtained in 20 ± 5% (n = 12) RCY within 90 min.

Quality Control. The quality control was performed with three consecutive batches of [^{18}F]DTG.

Organoleptic Test. The radiopharmaceutical preparation of [^{18}F]DTG was visually checked.

pH Determination. pH was determined with a pH paper (MN Duotest pH 1−12).

Chemical Identification, Purities, and Molar Activity Determination. Identification, purity, and MA determination were performed following the "liquid chromatography" monograph n°01/2019:20229 of the European Pharmacopoeia 11.5. A reverse-phase analytical HPLC system equipped with a 717_{plus} Autosampler system, a 1525 binary pump, a 2996 photodiode array detector (Waters, USA), and a Flowstar LB 513 (Berthold, France) gamma detector was used. The Empower 3 (Waters) software operated the equipment. A reverse-phase Symmetry C18 (150 mm × 3.9 mm, 5 μm, Waters) column was used with a mixture of H_2O/CH_3CN/PicB7 (70/30/0.2 v/v/v, 2 mL/min) as the eluent. UV detection was set at 254 nm. Comparison of the retention time of [^{18}F]DTG with the retention time of the non-radioactive DTG reference (t_R^{ref}) ensures chemical identification. Radiochemical and chemical purities were calculated as the ratio of the AUC of the DTG peak over the sum of the AUCs of all other peaks on gamma and UV chromatograms, respectively. MA was calculated as the ratio of the activity of the collected peak of [^{18}F]DTG measured in an ionization chamber (Capintec, Berthold) over the molar quantity of DTG determined using calibration curves. Radiochemical and chemical purities and molar activities are the mean values of three consecutive runs.

Residual Solvents. The content of residual acetone, acetonitrile, and ethanol was calculated according to the "Identification and control of residual solvents" monograph n°01/2017:20424 of the European Pharmacopoeia 11.5. The gas chromatograph (Clarus 580, PerkinElmer, USA) was equipped with a headspace injector (Turbomatrix 40, PerkinElmer, USA), a woot fused silica column (CP select 624 CB 30 m × 0.53 mm 3 μm, Varian, France), and a flame ionization detector. TotalChrom version 6 (PerkinElmer, USA) software was used to monitor the equipment. The headspace oven temperature was set at 80 °C, the transfer line temperature was set at 180 °C, the needle temperature was set at 120 °C, the oven temperature went from 40 to 140 °C, and the detector temperature was set at 250 °C. Helium was used as the vector gas (5 mL/min). Standard solutions of ethanol (5 mg/mL), acetone (5 mg/mL), and acetonitrile (4.1 mg/mL) were used. The maximum authorized concentrations were calculated for a 10 mL injection and compared to the results observed on the chromatogram of the [^{18}F]DTG preparation.

Residual DMI was measured by HPLC using a Synergi Polar-RP80A (250 × 46 mm, 4 μm) column (Phenomenex, France) and a mixture of CH_3CN/H_2O (9/1 v/v, 1.6 mL/min) as the eluent. UV detection was performed at 220 nm. Standard solutions of DMI (2−800 ng) were used to calibrate the measured areas under the curve at known concentrations. The resulting calibration curve was used to determine the residual concentration of DMI in the [^{18}F]DTG preparation.

Radionuclide Purity and Half-Life Determination. Radionuclide purity and half-life determination were assessed according to the "Radiopharmaceutical preparations" monograph n°07/2016:0125 of the European Pharmacopoeia 9.7 by gamma-ray spectrometry and radioactive decay measurement (gamma vision-32 V6.07 software, Ortec, France). Purity was assessed by the detection of the 511 keV gamma ray (>99.9%) on the gamma spectrum (up to a total peak energy of 1022 keV), and half-life was calculated by decay measurement during a 30 min period.

Li, Cu, and Sn Trace Quantification. Li, Cu, and Sn residues were quantitatively measured in three consecutive batches of [^{18}F]DTG by ICP-OES. These experiments were realized by Eurofins Quality Pharma Control SAS (France).

Filter Integrity. The "bubble point" test was applied to ensure the filter integrity according to the "Radiopharmaceutical preparations" monograph of the European Pharmacopoeia 11.5. The inlet side of the filter was connected to a compressed air supply with a needle dipped in water at the outlet side. The air pressure was increased gradually until a continuous stream of air bubbles in the water was observed.

Sterility. The sterility was assessed according to the "Sterility" monograph of the European Pharmacopoeia 11.5 by direct inoculation of resazurin thioglycolate, trypticase soy agar, and Sabouraud agar (Biomérieux, France) with an aliquot of the decayed preparation and incubation for 13 days at 32.5 °C for the first medium and 22.5 °C for the two others. Cultures were visually inspected and compared to positive and negative controls. Negative controls should be clear of any growth, while positive cultures should indicate growth.

Bacterial Endotoxins. 30 μL of the [^{18}F]DTG produced was diluted in 570 μL of a solution of LAL (Cambrex, USA), and the mixture was incubated for 60 min at 37 °C together with positive controls (solution of LAL with Gram-negative bacterial endotoxins at 20λ) and negative control containing only the LAL solution. After incubation, the tubes containing the solutions were flipped to check for the presence or absence of a gel formed at the bottom.

■ ASSOCIATED CONTENT

Supporting Information

The Supporting Information is available free of charge at https://pubs.acs.org/doi/10.1021/acsomega.4c05893.

^{1}H, ^{13}C NMR, and HRMS spectra of compound **2**; ^{1}H NMR spectra of compound **3**; LC/MS analysis of the deprotection reaction of **3**; radio-TLC analysis of the radiofluorination of **2**; calibration curve of the UV absorbance of DTG; residual solvent analysis of a [^{18}F]DTG batch; and radionuclide purity measurement of a [^{18}F]DTG batch (PDF)

https://doi.org/10.1021/acsomega.4c05893
ACS Omega 2024, 9, 41732−41741

AUTHOR INFORMATION

Corresponding Author

Fabien Caillé − *Université Paris-Saclay, Inserm, CNRS, CEA, Laboratoire d'Imagerie Biomédicale Multimodale Paris-Saclay (BioMaps), Orsay 91401, France;* orcid.org/0000-0003-0088-7337; Email: fabien.caille@cea.fr

Authors

Steve Huvelle − *Université Paris-Saclay, Inserm, CNRS, CEA, Laboratoire d'Imagerie Biomédicale Multimodale Paris-Saclay (BioMaps), Orsay 91401, France; Université Paris-Saclay, Inserm, CEA, Center for Immunology of Viral, Auto-immune, Hematological and Bacterial diseases (IMVA-HB/IDMIT), Fontenay-aux-Roses 92260, France*

Antoine Pinon − *Université Paris-Saclay, Inserm, CNRS, CEA, Laboratoire d'Imagerie Biomédicale Multimodale Paris-Saclay (BioMaps), Orsay 91401, France*

Christine Coulon − *Université Paris-Saclay, Inserm, CNRS, CEA, Laboratoire d'Imagerie Biomédicale Multimodale Paris-Saclay (BioMaps), Orsay 91401, France*

Thomas Bonasera − *GSK, Medicines Research Centre, Hertfordshire SG1 2NY, U.K.*

Catherine Chapon − *Université Paris-Saclay, Inserm, CEA, Center for Immunology of Viral, Auto-immune, Hematological and Bacterial diseases (IMVA-HB/IDMIT), Fontenay-aux-Roses 92260, France*

Thibaut Naninck − *Université Paris-Saclay, Inserm, CEA, Center for Immunology of Viral, Auto-immune, Hematological and Bacterial diseases (IMVA-HB/IDMIT), Fontenay-aux-Roses 92260, France*

Roger Le Grand − *Université Paris-Saclay, Inserm, CEA, Center for Immunology of Viral, Auto-immune, Hematological and Bacterial diseases (IMVA-HB/IDMIT), Fontenay-aux-Roses 92260, France*

Chris M. Parry − *ViiV Healthcare, London TW8 9GS, U.K.*

Bertrand Kuhnast − *Université Paris-Saclay, Inserm, CNRS, CEA, Laboratoire d'Imagerie Biomédicale Multimodale Paris-Saclay (BioMaps), Orsay 91401, France;* orcid.org/0000-0002-5035-4072

Complete contact information is available at: https://pubs.acs.org/10.1021/acsomega.4c05893

Notes

The authors declare the following competing financial interest(s): Thomas Bonasera is employed by GSK. Chris M. Parry is employed by ViiV Healthcare and has stock/shares in GSK.

ACKNOWLEDGMENTS

The authors thank the ANRS RHIVIERA and ViiV Healthcare for funding for this research.

REFERENCES

(1) Kandel, C. E.; Walmsley, S. L. Dolutegravir − a Review of the Pharmacology, Efficacy, and Safety in the Treatment of HIV. *Drug Des., Dev. Ther.* **2015**, *9*, 3547−3555.

(2) Jóźwik, I. K.; Passos, D.; Lyumkis, D. Structural Biology of HIV Integrase Strand Transfer Inhibitors. *Trends Pharmacol. Sci.* **2020**, *41* (9), 611−626.

(3) WHO. WHO recommends dolutegravir as preferred HIV treatment option in all populations, https://www.who.int/news/item/22-07-2019-Who-Recommends-Dolutegravir-as-Preferred-Hiv-Treatment-Option-in-All-Population (accessed Jul 22, 2019).

(4) Ambrosioni, J.; Levi, L.; Alagaratnam, J.; Van Bremen, K.; Mastrangelo, A.; Waalewijn, H.; Molina, J.-M.; Guaraldi, G.; Winston, A.; Boesecke, C.; Cinque, P.; Bamford, A.; Calmy, A.; Marzolini, C.; Martínez, E.; Oprea, C.; Welch, S.; Koval, A.; Mendao, L.; Rockstroh, J. K.; EACS, G. B. Major Revision Version 12.0 of the European AIDS Clinical Society Guidelines 2023. *HIV Med.* **2023**, *24* (11), 1126−1136.

(5) CDC. Guidelines and Recommendations|Clinicians|HIV|, https://www.cdc.gov/hiv/clinicians/guidelines/index.html (accessed Mar 04, 2024).

(6) Cahn, P.; Pozniak, A. L.; Mingrone, H.; Shuldyakov, A.; Brites, C.; Andrade-Villanueva, J. F.; Richmond, G.; Buendia, C. B.; Fourie, J.; Ramgopal, M.; Hagins, D.; Felizarta, F.; Madruga, J.; Reuter, T.; Newman, T.; Small, C. B.; Lombaard, J.; Grinsztejn, B.; Dorey, D.; Underwood, M.; Griffith, S.; Min, S. Dolutegravir versus Raltegravir in Antiretroviral-Experienced, Integrase-Inhibitor-Naive Adults with HIV: Week 48 Results from the Randomised, Double-Blind, Non-Inferiority SAILING Study. *Lancet* **2013**, *382* (9893), 700−708.

(7) Churchill, M. J.; Deeks, S. G.; Margolis, D. M.; Siliciano, R. F.; Swanstrom, R. HIV Reservoirs: What, Where and How to Target Them. *Nat. Rev. Microbiol.* **2016**, *14* (1), 55−60.

(8) Cory, T. J.; Schacker, T. W.; Stevenson, M.; Fletcher, C. V. Overcoming Pharmacologic Sanctuaries. *Curr. Opin. HIV AIDS* **2013**, *8* (3), 190−195.

(9) Kuo, H.-H.; Lichterfeld, M. Recent Progress in Understanding HIV Reservoirs. *Curr. Opin. HIV AIDS* **2018**, *13* (2), 137−142.

(10) Tisseraud, M.; Goutal, S.; Bonasera, T.; Goislard, M.; Desjardins, D.; Le Grand, R.; Parry, C. M.; Tournier, N.; Kuhnast, B.; Caillé, F. Isotopic Radiolabeling of the Antiretroviral Drug [18F]Dolutegravir for Pharmacokinetic PET Imaging. *Pharmaceuticals* **2022**, *15* (5), 587.

(11) Makaravage, K. J.; Brooks, A. F.; Mossine, A. V.; Sanford, M. S.; Scott, P. J. H. Copper-Mediated Radiofluorination of Arylstannanes with [18F]KF. *Org. Lett.* **2016**, *18* (20), 5440−5443.

(12) Chao, M. N.; Chezal, J.-M.; Debiton, E.; Canitrot, D.; Witkowski, T.; Levesque, S.; Degoul, F.; Tarrit, S.; Wenzel, B.; Miot-Noirault, E.; Serre, A.; Maisonial-Besset, A. A Convenient Route to New (Radio)Fluorinated and (Radio)Iodinated Cyclic Tyrosine Analogs. *Pharmaceuticals* **2022**, *15* (2), 162.

(13) Andersen, I. V.; García-Vázquez, R.; Battisti, U. M.; Herth, M. M. Optimization of Direct Aromatic 18F-Labeling of Tetrazines. *Molecules* **2022**, *27* (13), 4022.

(14) Hoffmann, C.; Kolks, N.; Smets, D.; Haseloer, A.; Gröner, B.; Urusova, E. A.; Endepols, H.; Neumaier, F.; Ruschewitz, U.; Klein, A.; Neumaier, B.; Zlatopolskiy, B. D. Next Generation Copper Mediators for the Efficient Production of 18F-Labeled Aromatics. *Chem.—Eur. J.* **2023**, *29* (2), No. e202202965.

(15) Budidet, S. R.; Dussa, N.; Kaki, G. R.; Yatcherla, S. R.; Sanapureddy, J. M. R.; Danda, S. R.; Katuroju, S.; Meenakshisunderam, S. An Improved Process for the Preparation of Dolutegravir. WO 2014128545 A2, 2014.

(16) Cai, Z.; Li, S.; Zhang, W.; Pracitto, R.; Wu, X.; Baum, E.; Finnema, S. J.; Holden, D.; Toyonaga, T.; Lin, S.; Lindemann, M.; Shirali, A.; Labaree, D. C.; Ropchan, J.; Nabulsi, N.; Carson, R. E.; Huang, Y. Synthesis and Preclinical Evaluation of an 18F-Labeled Synaptic Vesicle Glycoprotein 2A PET Imaging Probe: [18F]-SynVesT-2. *ACS Chem. Neurosci.* **2020**, *11* (4), 592−603.

(17) Council of Europe *General Monograph 0125 - Radiopharmaceutical Preparations In European Pharmacopoeia*; Council of Europe: Strasbourg, 2023.

(18) Burt, T.; Young, G.; Lee, W.; Kusuhara, H.; Langer, O.; Rowland, M.; Sugiyama, Y. Phase 0/microdosing Approaches: Time for Mainstream Application in Drug Development? *Nat. Rev. Drug Discovery* **2020**, *19* (11), 801−818.

(19) Lo, C. C.; Chao, P. M. Replacement of Carcinogenic Solvent HMPA by DMI in Insect Sex Pheromone Synthesis. *J. Chem. Ecol.* **1990**, *16* (12), 3245−3253.

(20) ICH Q3D-R2 Guidelines. https://database.ich.org/sites/default/files/Q3D-R2_Guideline_Step4_2022_0308.pdf (accessed Nov 28, 2023).

https://doi.org/10.1021/acsomega.4c05893
ACS Omega 2024, 9, 41732−41741